International Journal of General Medicine Dovepress

Open Access Full Text Article ORIGINAL RESEARCH

Bioinformatics Analysis and Experimental Validation of Endoplasmic Reticulum Stress-Related Genes in Osteoporosis

Yong Zheng, Yonggui Luo, Kuihan Tang

Department of Orthopedics, Beijing Jishuitan Hospital Guizhou Hospital, Guiyang, 550014, People's Republic of China

Correspondence: Kuihan Tang, Email tkh5200520@163.com

Background: Endoplasmic reticulum stress (ERS) is closely associated with Osteoporosis (OP). In order to explore the role of ERS related genes in OP and its molecular mechanism.

Methods: OP-related transcriptome data were retrieved from the Gene Expression Omnibus (GEO) database. Weighted gene co-expression network analysis (WGCNA) was applied to screen OP-related genes. Differentially expressed ERS-related genes (DE-ERSGs) between OP and controls were identified by overlapping OP-related, differentially expressed genes (DEGs), and ERS-related genes. ERS-related genes. Gene Ontology (GO) and Kyoto Encyclopedia of Genes and Genomes (KEGG) analyses were conducted to explore their functions. Receiver operating characteristic (ROC) curves assessed the diagnostic value of DE-ERSGs, and comparative toxicogenomics database (CTD) was used to predict targeting agents for key DE-ERSGs. Finally, biomarker expression was verified by real time quantitative polymerase chain reaction (RT-qPCR).

Results: A total of 10 DE-ERSGs were screened in OP patients. GO and KEGG analyses indicated their enrichment in Alcoholic liver disease, Endometrial cancer, and Glycerolipid metabolism. ROC curve analysis revealed that RPN2, FOXO3, ERGIC2, and MYO9A had significant diagnostic value, thus being identified as key DE-ERSGs. Moreover, the key DE-ERSGs-drug interaction network showed that some drugs such as bisphenol A, Cisplatin, Cyclosporine, and Valproic Acid might play roles by targeting key DE-ERSGs in OP. The expression validation analysis of key DE-ERSGs revealed that RPN2, ERGIC2, and MYO9A was significantly expressed in the GSE62402. Ultimately, The blood samples RT-qPCR verification results show that RPN2, ERGIC2, and MYO9A were significantly lower in OP samples compared to normal samples ($p < 0.05$), whereas there was no difference in the expression levels of FOXO3.

Conclusion: RPN2, FOXO3, ERGIC2 and MYO9A as the biomarkers associated with ERS in OP by bioinformatics analysis, which may provide new biological targets for clinical treatment.

Keywords: osteoporosis, endoplasmic reticulum stress, bioinformatics analysis, biomarkers

Introduction

Osteoporosis (OP) is a common metabolic bone disease in clinical practice, which is characterized by bone microstructure destruction, decreased bone mineral density and increased bone fragility. Fracture is one of its common complications.[1] Investigation and research found that the incidence of women over 50 years old is higher than that of men, which poses a great threat to people's life and health.[2] As an age-related chronic disease, has the characteristics of high incidence, high treatment cost, high disability rate, long course of disease, long course of treatment, low quality of life, and insufficient social attention.[3] How to detect fragility fracture early, prevent it and improve the quality of people's life has become an important public health issue in the world.

Endoplasmic reticulum (ER) is a membrane-sealing organelle with multiple functions. Some of its major functions are co-translational transport, modification, folding, and processing of secretory, lysosomal, and transmembrane

Received: 12 July 2024
Accepted: 27 October 2024
Published: 18 November 2024

proteins,[4] namely processes involving multiple enzymes and ER chaperones.[5] Endoplasmic reticulum in cells more than a third of the protein synthesis, folding and structure plays an important role in the process of mature.[6]

The normal function of endoplasmic reticulum need not folded protein synthesis in the endoplasmic reticulum and endoplasmic reticulum partner active balance between.[4] When overload endoplasmic reticulum protein folding ability, breaking the balance between partners and the endoplasmic reticulum, cells can produce endoplasmic reticulum stress.[7] Studies have found that endoplasmic reticulum stress and continuous UPR signal transduction are closely related to the occurrence and development of diabetes, neurodegeneration, stroke, pulmonary fibrosis, viral infection, inflammatory diseases, cancer and heart disease.[8] ER stress (ERS) is triggered by various metabolic factors, such as cholesterol and proinflammatory cytokines. Recent studies have shown that endoplasmic reticulum stress is closely related to OP and other bone diseases. It has been reported that endoplasmic reticulum stress can inhibit bone formation through the expression of Activating Transcription Factor C/EBP homologous protein CHOP signaling pathway, thus leading to OP.[9] In addition, endoplasmic reticulum stress can regulate osteoclast activity through signaling molecule PERK, thus leading to OP.[10]

However, the molecular mechanisms by which the ER mediates OP have not been elucidated. As a high-throughput and efficient sequencing technology, gene microarray analysis is widely used to screen for important genetic or epigenetic changes in the development of various diseases and to identify biomarkers related to diagnosis or assessment of patient prognosis.[11]

To sum up, this study aimed to screen out the ERS related genes in OP patients through the analysis of bioinformatics, such as differential expression analysis and Weighted gene co-expression network analysis (WGCNA). Our findings explored the influence and molecular mechanisms of ERS-related genes in OP, attempted to identify diagnostic markers and provide a theoretical basis for the invention of the drug, which is of great significance for the study of the pathogenesis and prevention of OP.

Materials and Methods

Data Extraction

The transcriptomic data associated with OP were obtained from the Gene Expression Omnibus (GEO) (GSE56815 and GSE62402) database (https://www.ncbi.nlm.nih.gov/geo/). The GSE56815 dataset, containing blood tissues from 40 high bone mineral density (BMD) and 40 low BMD samples, was used for WGCNA network construction and DE-ERSGs screening; the GSE62042 dataset, including blood tissues from 5 high BMD and 5 low BMD samples, was applied to validate the expression of DE-ERSGs. Additionally, we obtained 1448 ERSGs from the Genecards database (https://www.genecards.org/). Clinical information for patients with GSE56815 and GSE62402 was provided in Supplementary Tables 1 and 2.

WGCNA

The gene-expression profiles form GSE56815 dataset were applied to explore the OP-related module using the "WGCNA" R package (version 1.70–3).[12] Firstly, an adjacency matrix was constructed to describe the correlation strength between the nodes based on the formula of the adjacency matrix:[13]

$$s_{ij} = \left|\mathrm{cor}\left(X_i, X_j\right)\right| a_{ij} = s_{ij}\beta$$

in which i and j denote two different genes, x_i and x_j represent expression values. S_{ij} denotes the correlation coefficient, and a_{ij} represents the strength of the correlation between i and j. In the study, we construct the adjacency matrix with optimal soft-threshold power (β) set to 8 and scale-free topological index set to 0.85. Subsequently, we convert the adjacency matrix into a topological overlap matrix. Finally, hierarchical clustering trees with modules are formed by dynamically cutting trees to identify key modules by introducing genes with similar expression patterns into the same module.

Differential Expression Analysis

Firstly, differentially expressed genes (DEGs) between high BMD samples and low BMD samples were detected in the GSE56815 dataset utilizing the "limma" R package (version 3.46.0)[14] with an adjusted $p<0.05$. Meanwhile, the DEGs obtained above were intersected with ERSGs and key module genes using the "VennDiagram" R package (version 1.6.20)[15] to obtain DE-ERSGs for this study. Subsequently, GO functional and KEGG pathway enrichment analyses of the DE-ERSGs were performed using the "clusterProfiler" R package.[16,17]

Identification and Validation of Key DE-ERSGs

The "pROC" R package[18] (version 1.17.0.1) was applied to graph the ROC curve to assess and validate the diagnostic value of DE-ERSGs in the GSE56815 and GSE62402 datasets, respectively, and select genes with high diagnostic value as key DE-ERSGs. Then, the expression value of these key DE-ERSGs was verified in the GSE62402 dataset.

Gene Set Enrichment Analysis (GSEA)

In order to delve deeper into the potential biological functions of the key DE-ERSGs in the patient population, correlation coefficients between each key gene and all the genes in the training set GSE56815 were calculated using the R package "psych" (version 2.4.3).[19] Subsequently, these correlation coefficients were sorted in descending order, generating corresponding gene ranking lists for each prognostic gene. Then, GSEA was conducted on these sorted gene lists using the R package "clusterProfiler" (version 4.10.1).[16] During the enrichment analysis, a P-value threshold of <0.05 was adopted to identify the most significant pathways. Ultimately, the top 5 most significant pathways were selected for visualization. The reference gene set used in the analysis was downloaded from the Molecular Signatures Database (MSigDB) (https://www.gsea-msigdb.org/gsea/msigdb) as "c2.cp.kegg.v7.4.symbols.gmt".

Prediction of Potential Therapeutic Agents for DE-ERSGs

The CTD website (https://dgidb.genome.wustl.edu) was applied to predict target drugs for key DE-ERSGs to identify small molecule compounds with potential therapeutic effects in OP patients.

RT-qPCR Analysis

Blood samples (10 OP group samples and 10 control group samples) were obtained from OP patients and normal samples with their knowledge and consent from Beijing Jishuitan Hospital Guizhou Hospital, and this study was approved by the Beijing Jishuitan Hospital Guizhou Hospital ethics committee, all methods were performed in accordance with relevant guidelines and regulations in the Ethical considerations in the review of biomedical research involving human subjects and the Declaration of Helsinki. The expression of the key DE-ERSGs was further validated via RT-qPCR. Twenty freshly collected blood samples were subjected to the isolation of PBMCs (Peripheral Blood Mononuclear Cells). Initially, an equal volume of PBMC separation medium was added to 15mL centrifuge tubes, followed by the slow addition of well-mixed whole blood (with each sample not exceeding 3 mL; if less, it was supplemented to 3 mL). After centrifuging at 2000g for 20 minutes, the liquid was visibly divided into four layers, with PBMCs present in the second, milky white, ring-shaped layer. Subsequently, the PBMC layer was carefully aspirated into a new centrifuge tube, and PBS was added to 15 mL to resuspended the cells. After another centrifugation at 1000g for 10 minutes, the supernatant was discarded. Then, 1 mL of TRIzol (Ambion, Austin, USA) was added, and the mixture was allowed to stand at room temperature for 10 minutes to lyse the cells, followed by storage in a −80°C freezer for future use. Total RNA of 20 samples were extracted using TRIzol (Ambion, Austin, USA) according to the instructions provided by the manufacturer. The extracted RNA was reverse transformed into cDNA using the method of the SureScript-First-strand-cDNA-synthesis -kit before RT-qPCR. RT-qPCR was performed utilizing the 2xUniversal Blue SYBR Green qPCR Master Mix (Servicebio, Wuhan, China). The primer sequences for PCR were shown in Table 1. The GAPDH gene served as an internal control, and the relative expression of biomarkers was determined using the $2^{-\Delta\Delta Ct}$ method.

Table 1 The Primer Sequences for PCR

Primer	Sequence
FOXO3 F	GGCCCGGGATAACCAACTCT
FOXO3 R	CTCCACTTCGAGCGGAGAGA
ERGIC2 F	GGACCATAACACAAGCATGAC
ERGIC2 R	TCAGGAACCTTCGGAAAGGC
MYO9A F	CCTGACACCACTGACCCACTAC
MY09A R	AACCGAACTACAACAGGAGACG
RPN2 F	GCCGAGCCAGACAACAAGAAC
RPN2 R	TGGGACAAGACAGTCGAGGGA
Internal control-GAPDH F	CGAAGGTGGAGTCAACGGATTT
Internal control-GAPDH R	ATGGGTGGAATCATATTGGAAC

Statistical Analysis

All statistical analyses and visual plotting of the results were performed based on R software (https://www.r-project.org/, version 4.0.3). Correlation coefficients and p-values were calculated for key modules and OP patients using Pearson correlation analysis. The P-value<0.05 was considered statistically significant.

Results

Identifiction of the OP-Related Modules and Genes Through WGCNA

To identify OP-related modules and genes, WGCNA was applied to build the co-expression network using all samples and genes in the GSE56815 dataset. A sample dendrogram was constructed to detect and remove 3 outliers (Figure 1A). Then, a scaleless network was construct with the optimal soft-threshold power (β) was set as 8 and the index of scale-free topologies was set as 0.85 (Figure 1B). A hierarchical clustering tree with modules was formed by introducing genes with similar expression patterns into the same module by a dynamic tree-cutting, and 16 modules were identified (Figure 1C). Among 16 modules, MEpink (|Cor|>0.3, p<0.05), MEred (|Cor|>0.3, p<0.05), and MEblack (|Cor|>0.3, p<0.05) had the highest correlation with high and low BMD groups (Figure 1D). Therefore, these three modules and 326 genes in these three modules were finally used for the subsequent analysis.

Identification of DE-ERSGs

To screen DE-ERSGs, we firstly screened DEGs between high BMD samples and low BMD samples in the GSE56815 dataset. A total of 433 DEGs, including 300 down-regulated and 133 up-regulated in OP samples, were identified (Figures 2A and B). Then, 10 DE-ERSGs were obtained for subsequent analysis by intersecting DEGs, key module genes, and ERSGs (Figure 2C).

GO and KEGG Analysis of DE-ERSGs

We then performed GO and KEGG analysis to determine the role of the 10 DE-ERSGs in biological process. The results of GO enrichment analysis suggested that these DE-ERSGs were mainly involved in 5 terms such as cellular lipid catabolic process, oocyte development, and regulation of myelination in biological process (BP). In molecular function (MF), these DE-ERSGs were mainly involved in transcription coregulator binding and beta-catenin binding. In cellular component (CC), these DE-ERSGs were mainly involved in endoplasmic reticulum-Golgi intermediate compartment membrane, COPII-coated ER to Golgi transport vesicle, melanosome, and pigment granule (Figure 3A). Furthermore, in KEGG terms, these DE-ERSGs were significantly associated with Alcoholic liver disease, Endometrial cancer, and Glycerolipid metabolism, etc. pathways (Figure 3B and Supplementary Table 3).

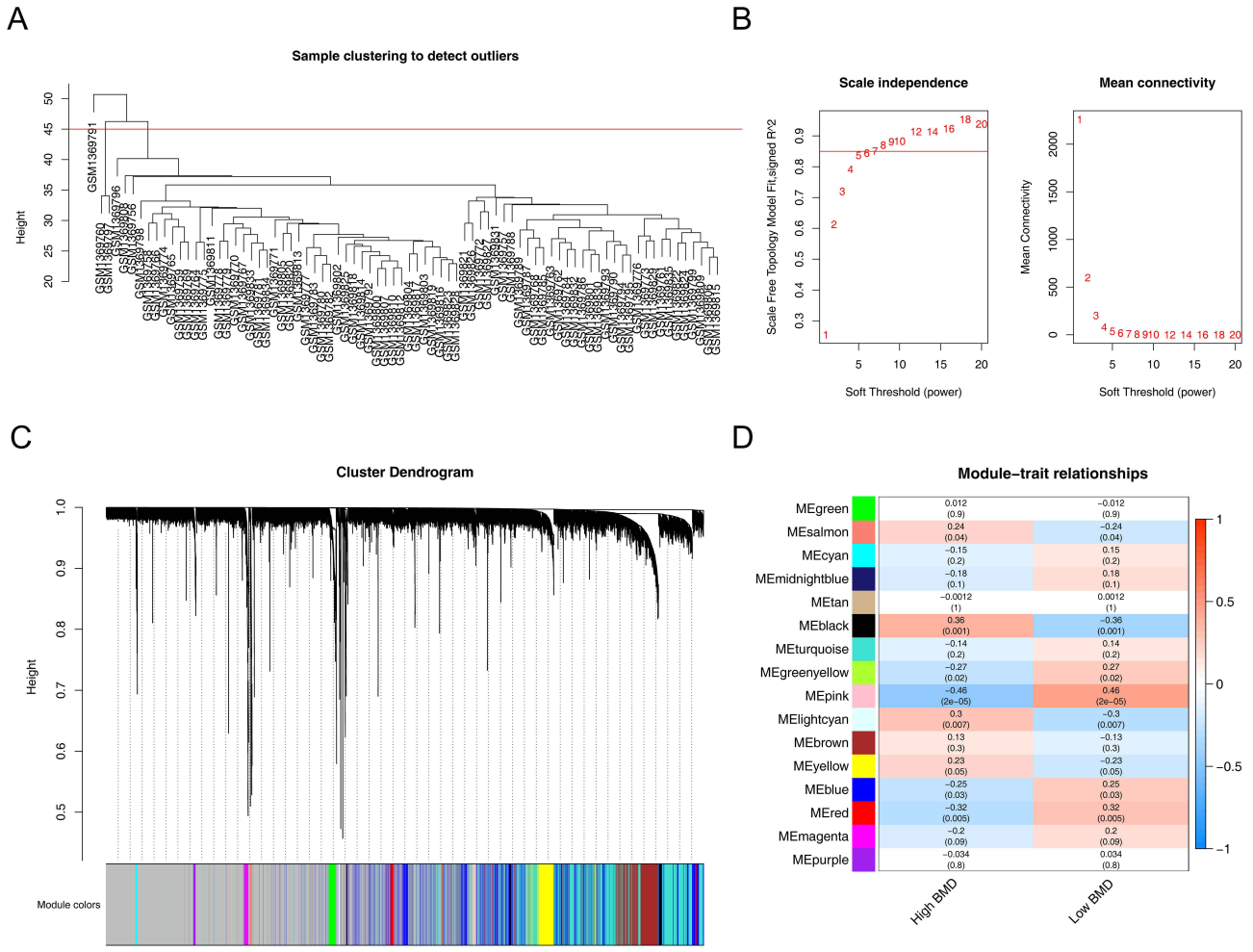

Figure 1 A total of 326 osteoporosis (OP)-related genes were acquired by Weighted Gene Co-expression Network Analysis (WGCNA). (**A**) The sample clustering tree established to recognize the outlier samples. (**B**) The scale-free fit exponent of the soft threshold power and average degree of connectivity. (**C**) Hierarchical clustering of genes and module identification. (**D**) The heatmap of the relationships between gene modules and clinical traits. Positive correlations are shown in red and negative correlations in blue.

Identification and Verification of Key DE-ERSGs

To further explore the diagnostic and expression value of 10 DE-ERSGs, we firstly evaluated and validated the diagnostic value of these DE-ERSGs in the GSE56815 and GSE62402 datasets, respectively. As shown in Figure 4A, 9 of these DE-ERSGs (RAC1, RPN2, FOXO3, GLA, ABCD4, LPIN2, ERGIC2, SEC22B, and MYO9A) have AUC values greater than 0.7 in the GSE56815 dataset. It was verified that RPN2, FOXO3, ERGIC2, and MYO9A of these DE-ERSGs had a AUC value greater than 0.7 in the GSE62402 dataset (Figure 4B). Therefore, these 4 genes were identified as key DE-ERSGs. Subsequently, we also assessed and verified the expression value of the 4 key DE-ERSGs, and the results showed that the trend of RPN2, ERGIC2, and MYO9A expression dysregulation was consistent in the training and validation sets (Figures 4C and D).

Gene Set Enrichment Analysis (GSEA) of Key DE-ERSGs

Through GSEA, the potential biological functions of four key DE-ERSGs (RPN2, FOXO3, ERGIC2, and MYO9A) were explored. The results indicated that RPN2 was co-enriched in 17 pathways, including ribosome, proteasome, oxidative phosphorylation, parkinsons disease, and selenoamino acid metabolism (Figure 5A). FOXO3 was mainly enriched in 17 pathways such as hypertrophic cardiomyopathy, dilated cardiomyopathy, pantothenate and CoA Biosynthesis, proteasome, and RNA degradation (Figure 5B). ERGIC2 was co-enriched in 44 pathways, with the top 5 being neuroactive ligand receptor interaction, proteasome, spliceosome, dilated cardiomyopathy, and calcium signaling pathway (Figure 5C). MYO9A was

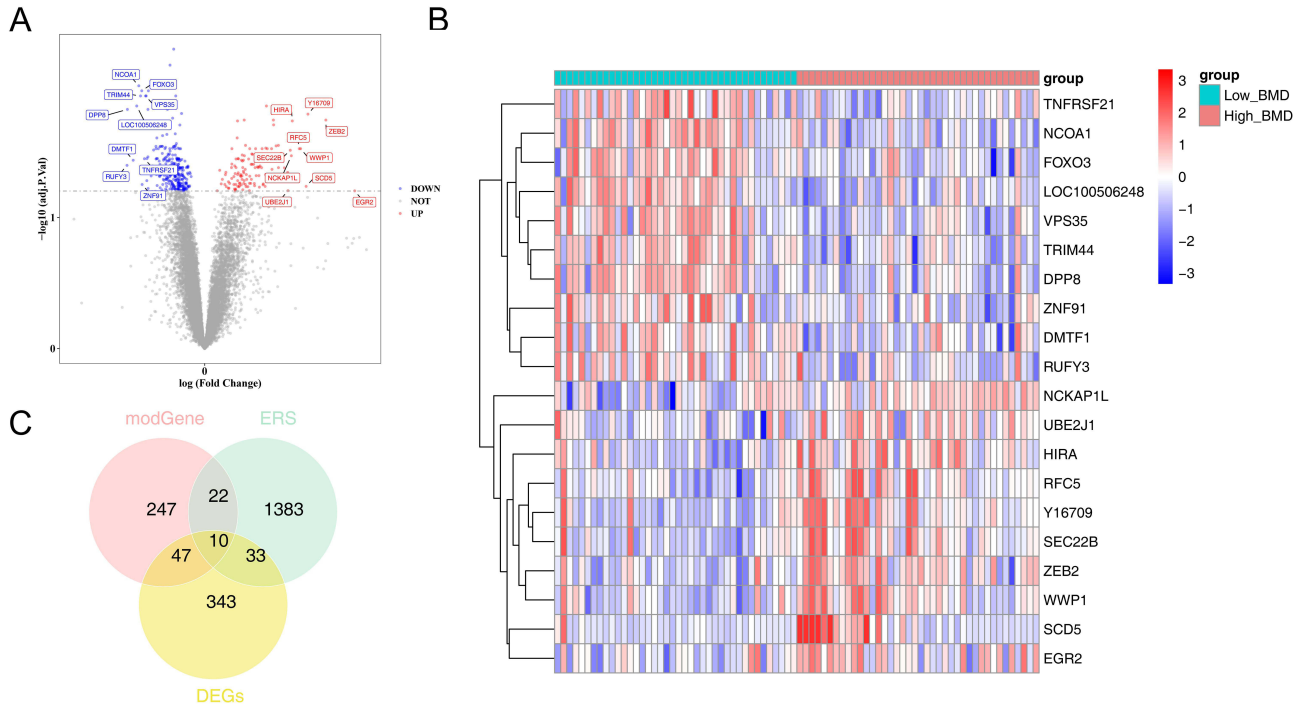

Figure 2 Differential expression analysis in the GSE56815 dataset. (**A** and **B**) The volcano map (**A**) and heatmap (**B**) of differentially expressed genes (DEGs) between high bone mineral density (BMD) and low BMD samples. (**C**) The venn diagram of differentially expressed endoplasmic reticulum stress related genes (DE-ERSGs).

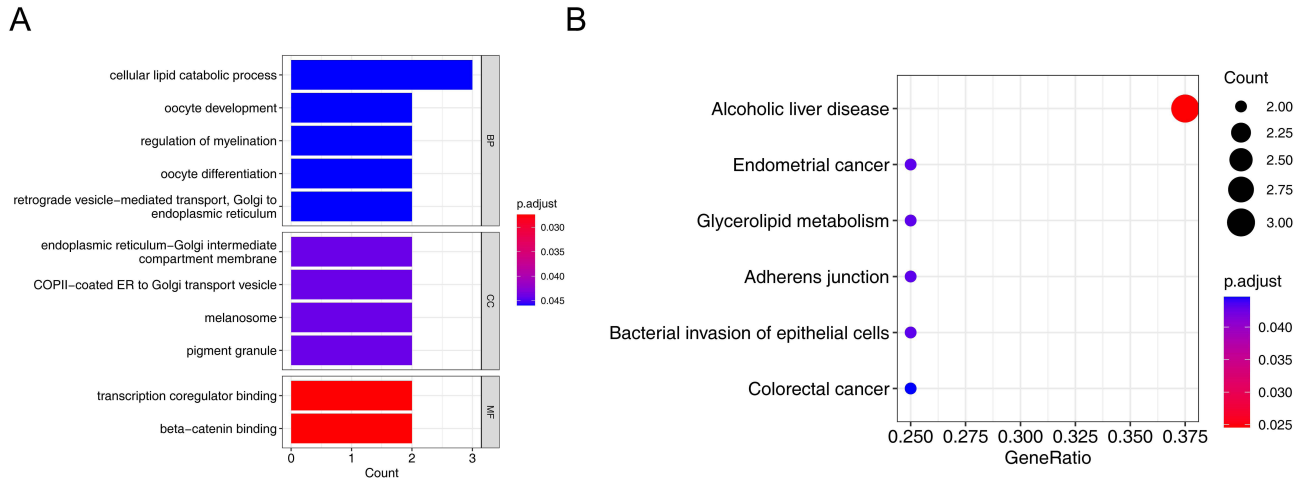

Figure 3 Exploration of potential functions of DE-ERSGs. (**A**) The bar chart of Gene Ontology (GO) terms enriched in DE-ERSGs. BP, biological progress; CC, cellular component; MF, molecular function. (**B**) The bubble chart of Kyoto Encyclopedia of Genes and Genomes (KEGG) pathways enriched in DE-ERSGs.

primarily enriched in 30 pathways, including pathogenic Escherichia coli infection, chronic myeloid leukemia, neuroactive ligand receptor interaction, Fc gamma R-mediated phagocytosis, and ubiquitin-mediated proteolysis (Figure 5D).

Prediction of Potential Therapeutic Agents for Key DE-ERSGs

The CTD web server was utilized to predict targeting agents for key DE-ERSGs and to identify small molecule compounds with potential therapeutic effects in OP patient. As shown in Figure 6, 8 drugs such as bisphenol A, vinclozolin, and sodium arsenate are interrelated with the RPN2; 19 drugs such as Cisplatin, Doxorubicin, and Ethanol are interrelated with the FOXO3; 4 drugs (bisphenol A, Cyclosporine, sodium arsenate, and Valproic Acid) are

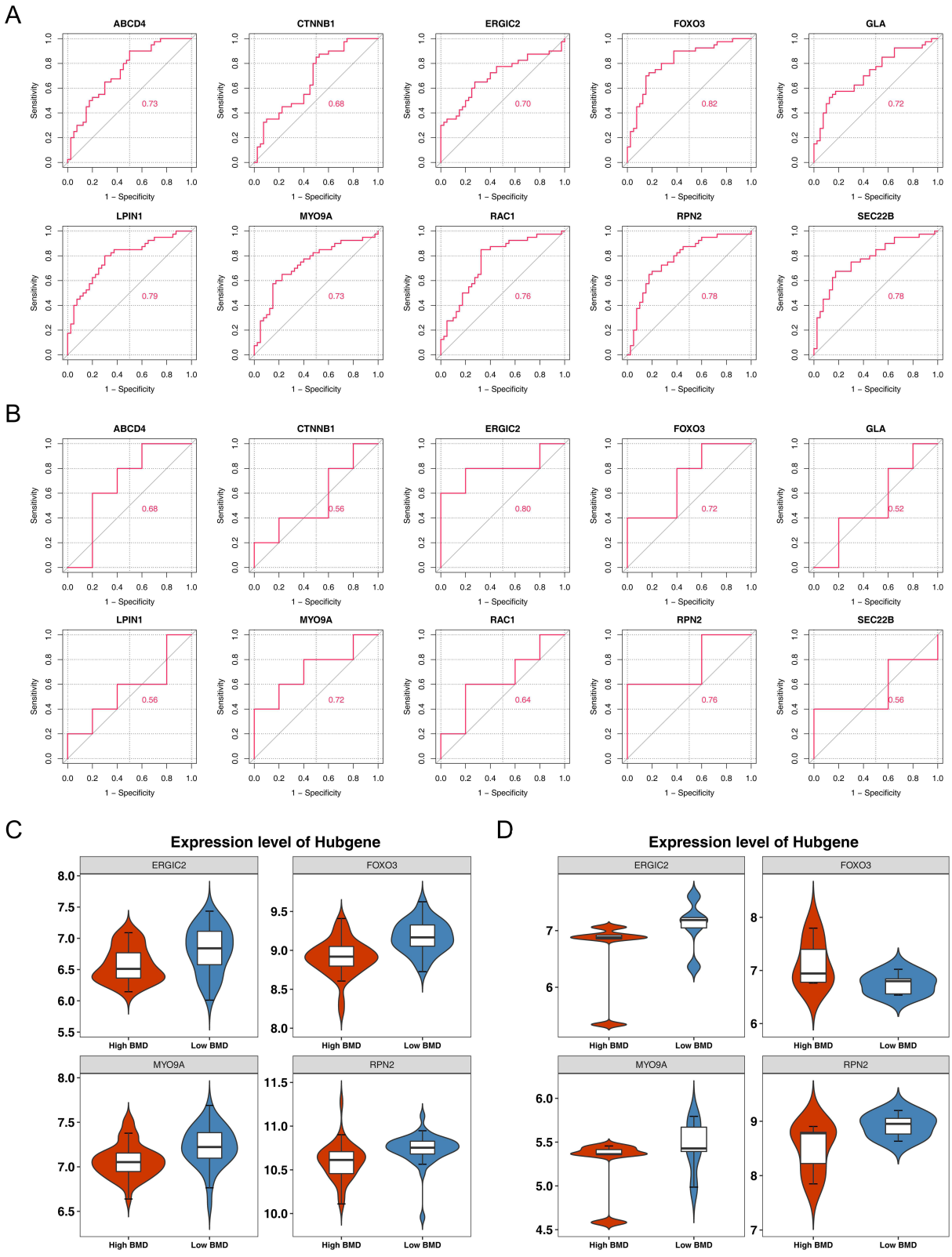

Figure 4 The assessment of diagnostic value and expression discrepancies for DE-ERSGs. (**A** and **B**) The receiver operating characteristic (ROC) curves of DE-ERSGs in the GSE56815 (**A**) and GSE62402 (**B**) datasets. The greater the area under the curve (AUC) value, the greater the ability to distinguish between high BMD and low BMD groups. (**C** and **D**) The expression levels of key DE-ERSGs in high BMD and low BMD samples in the GSE56815 (**C**) and GSE62402 (**D**) datasets.

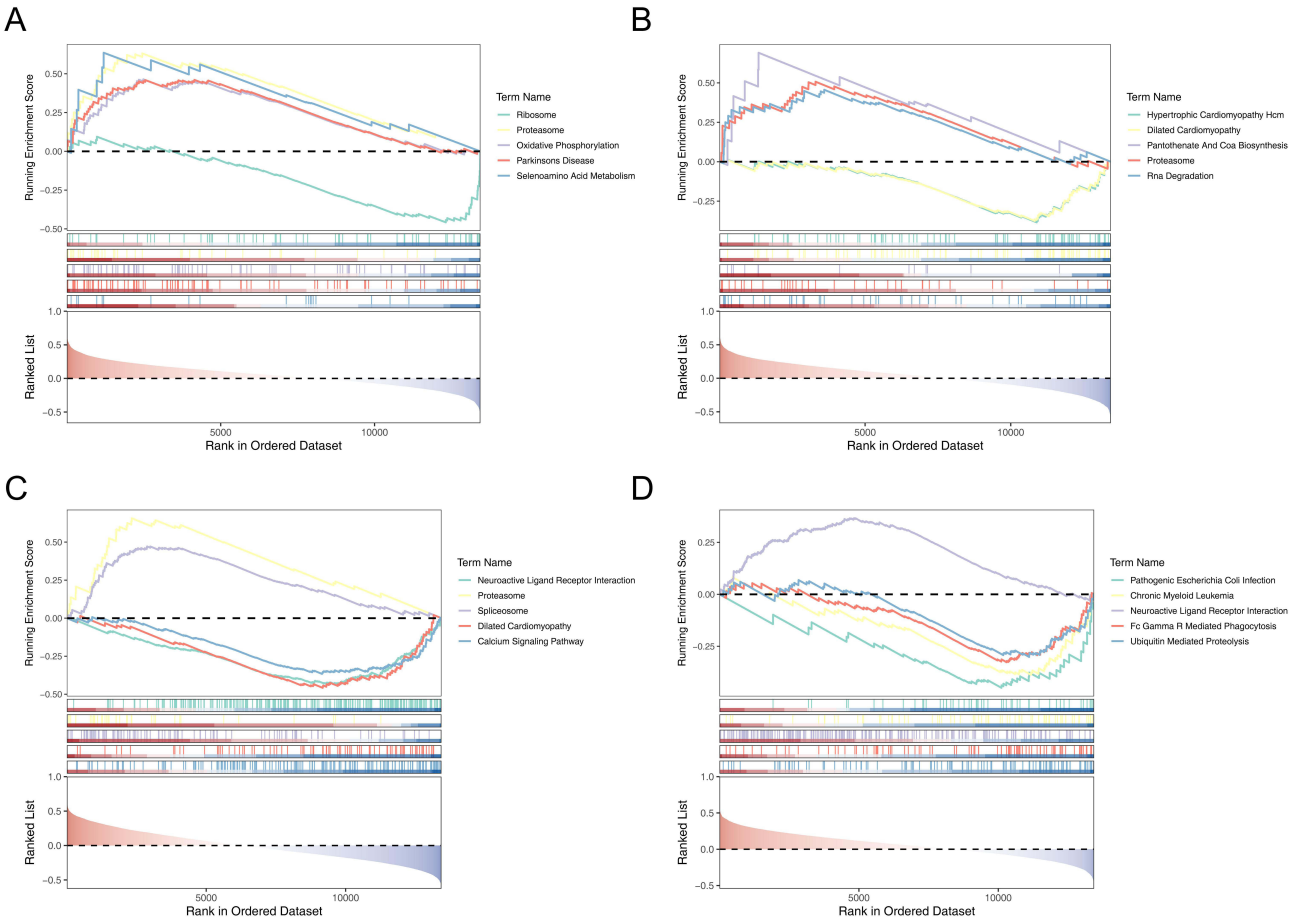

Figure 5 Results of GSEA enrichment analysis. (**A**) Results of GSEA enrichment analysis of RPN2. (**B**) Results of GSEA enrichment analysis of FOXO3. (**C**) Results of GSEA enrichment analysis of ERGIC2. (**D**) Results of GSEA enrichment analysis of MYO9A.

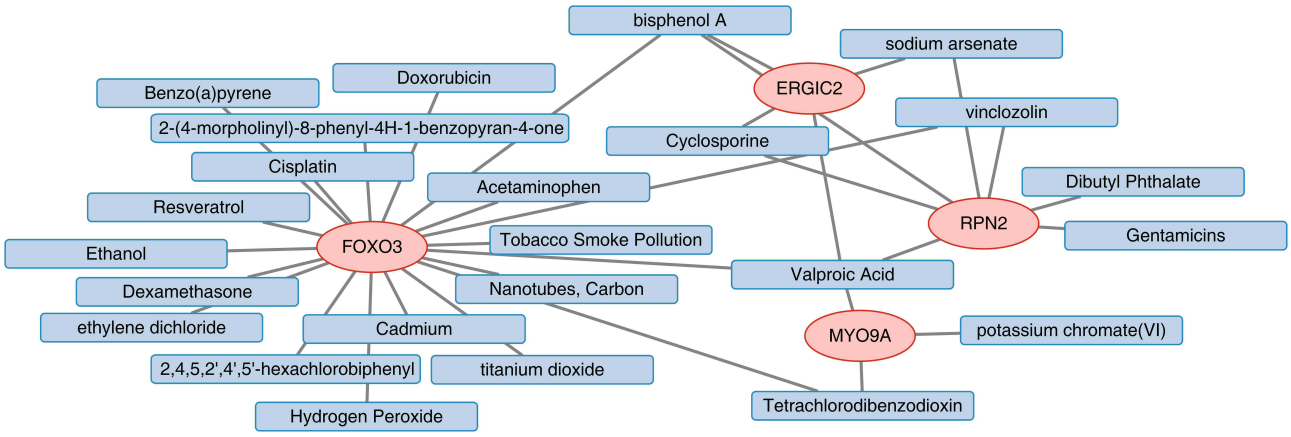

Figure 6 Key gene-drug interaction network. Pink ovals represent key DE-ERSGs and blue rectangles represent targeted drugs.

interrelated with the ERGIC2; 3 drugs, including Valproic Acid, Tetrachlorodibenzodioxin, and potassium chromate (VI), are interrelated with the MYO9A.

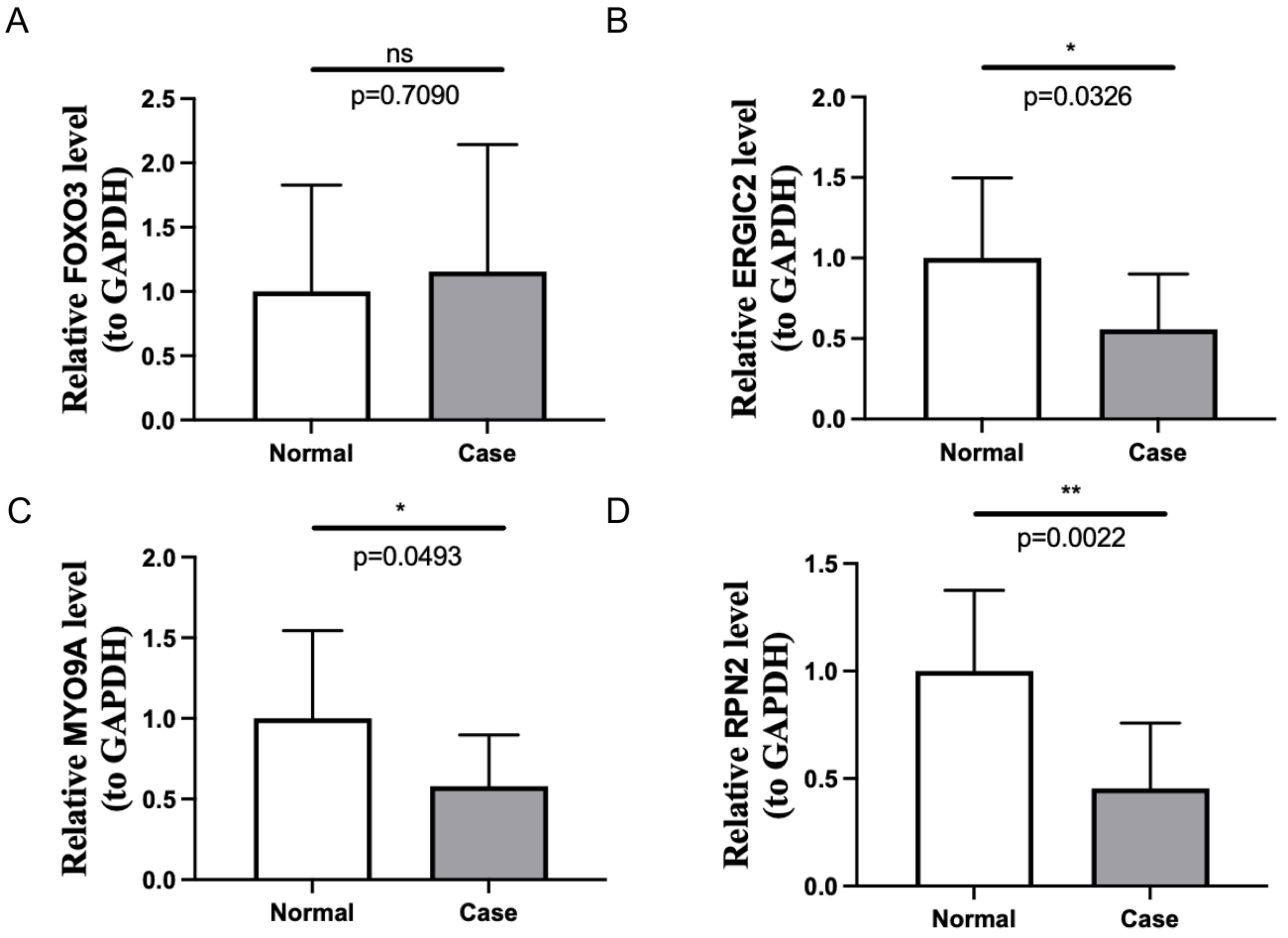

Figure 7 Validation of the expression of four key DE-ERSGs in OP and control samples by RT-qPCR. The RT-qPCR validation results shown in the figure were based on ten samples from the OP group and ten samples from the control group. (**A**) FOXO3; (**B**) ERGIC2; (**C**) MYO9A; (**D**) RPN2. ns, not significant; *p<0.05; **p<0.01.

The Expression Levels of the Key DE-ERSGs

RT-qPCR results showed that the trends of key DE-ERSGs in the OP and control groups were the same as in the training and validation sets (Figure 7). The expression levels of key DE-ERSGs RPN2, ERGIC2, and MYO9A were significantly lower in OP samples compared to normal samples, whereas there was no difference in the expression levels of FOXO3.

Discussion

OP is a systemic bone disease that is common in middle-aged and elderly people. It is the feature of bone microstructure damage and bone mass decreases, resulting in increased fracture risk.[20] As a worldwide epidemic, according to statistics, there are more than 200 million OP patients in the world.[21] So far, the mechanism of the OP occurrence is not clear. ERS plays a key role in the pathogenesis of OP, and mediates through a variety of ways. For example, Hamamura et al regulate osteoblast function through endoplasmic reticulum stress to affect osteogenesis.[22] Chen et al[23] increase bone loss by enhancing osteoclast activity, and ERS has a bidirectional regulation effect on bone marrow mesenchymal stem cells.[24–26] Han[27] alleviates OP by targeting the inhibition of endoplasmic reticulum stress to channel collaterality. However, the mechanism of action of ERS related genes in OP is uncertain, and it is worth to exploring.

In this study, transcriptome data related to osteoporosis (OP) were obtained from GEO and OP-related genes were screened using WGCNA. Subsequently, by comparing OP-related differentially expressed genes (DEGs) with those associated with ER stress (ERS), we identified 10 ERS-related genes (DE-ERSGs) that were differentially expressed between OP and control. Further use of GO and KEGG revealed the functional enrichment of these genes in alcoholic liver disease, endometrial cancer, and triglyceride metabolism. ROC curve analysis showed that RPN2, FOXO3,

ERGIC2 and MYO9A had significant diagnostic value and were identified as key DE-ERSGs. In addition, key DE-ersGs -drug interaction network analysis suggests that drugs such as bisphenol A, cisplatin, cyclosporine, and valproic acid may work by targeting key DE-ERSGs in OP. Next, we used the GSE62402 dataset and RT-qPCR validation to finally identify RPN2, FOXO3, ERGIC2, and MYO9A as ERS related biomarkers in OP, and these findings may provide new biological targets for clinical treatment.The highly conserved RPN2 is present only in the rough endoplasmic reticulum membranes and is involved in the translocation of secreted proteins and the maintenance of the inherent distinctiveness of the rough endoplasmic reticulum.[28,29] Earlier studies showed that the oligosaccharide transferase complex contains RPN2 protein and binds the N-X-S/T common motif of oligosaccharide and asparagine residue polypeptide chains.[30,31] Studies have shown that overexpression of RPN2 enhances osteogenic differentiation, and RPN2 silencing of hBMSCs is thought to be closely related to the down-regulation of certain osteogenesis-related genes, matrix mineralization, and ALP function. RPN2 may serve as a potential marker for osteogenic differentiation.[32] FOXO belongs to the forked head transcription factor family, which is characterized by a DNA binding motif with a winged helix (the so-called forked head domain). FOXO3 is one of the subtypes.[33] FOXO3 was mainly expressed in heart, brain, kidney, ovary and bone.[34,35] Overexpression of FOXO3 in mature osteoblasts reduced oxidative stress and osteoblast apoptosis, and increased the number of osteoblasts, bone formation rate and vertebral bone mass,[36,37] and FOXO3 could up-regulate ALP to promote bone formation.[33] OP and other bone diseases occur as a result of disruption of intercellular communication within the basic multicellular unit (BMU).[38] FOXO3 was also involved in the regulation of oxidative stress-induced autophagy in bone cells, including osteoblasts, osteocytes and osteoclasts.[39] Knockout of FOXO1, 3, and 4 in mice has been reported to result in reduced expression of Runx2, Osterix, and alkaline phosphatase in in vitro osteogenic precursor cells, as well as a significant reduction in the number of cell colony forming unit (CFU) fibroblasts and CFU osteoblasts in the bone marrow of these mice. This implies that FOXO protein can regulate the differentiation and proliferation of osteoblasts.[40] In summary, FOXO3 can promote osteogenic differentiation.

ERGIC2 (formerly known as PTX1) is a gene identified in our laboratory by subtractive hybridization on the basis that it was expressed in normal prostate, but not in prostate carci-Noma.[41] This suggested that the ERGIC2 protein was an endoplasmic reticulum (ER) resident protein involved in protein transport between the ER and the Golgi intermediate compartment (ERGIC) and the cis-Golgi.[42] It was closely related to the development of mandible, hip bone, femur and knee joint.[43] Furthermore, they showed that the recombi-nant ERGIC2 protein interacted with protein elongation factor-1a, which has a protective function against ER stress-induced apoptosis.[42]

Unconventional myosin is an actin based molecular motor that is present in almost all eukaryotic cells. There are two kinds of 9 types of myosin expression in human body; MYO9A and MYO9B. Studies have shown that MYO9A has a role in maintaining the cytoskeleton of neurons, and have demonstrated adverse downstream effects of MYO9A on vesicle transport and protein secretion.[44] MYO9A is associated with congenital muscle weakness and joint contracture.[45,46]

Previous studies have shown that the ribosome pathway is a potential pathway to regulate OP process.[47] On the basis of OP, metabolic factors may further accelerate the development of osteoarthritis (OA), especially in osteoporotic OA. When ErXian Decoction (EXD) was used for beneficial intervention, it was found that the mechanism of action involved cysteine, andeoxycholic acid and D-trehalose, which were closely related to key metabolic pathways such as glycolysis/ gluconeogenesis, pantothenic acid metabolism and coenzyme A (CoA) biosynthesis. More importantly, the bioanabolic pathway of CoA has a significant impact on OP, which may have a positive effect on the pathological evolution of OP through fine regulation of related metabolic processes, and thus help to alleviate or delay the progression of osteoporotic OA.[48] In addition, neuroactive ligand-receptor interactions, cyclic adenosine phosphate (cAMP) signaling pathway and calcium signaling pathway are closely related to articular cartilage degradation, bone formation and bone resorption processes. In particular, neuroactive ligand-receptor interactions are seen as one of the important mechanisms by which Xianling Gubao (XLGB) capsules act on OP, suggesting that it may play an integral role in regulating bone health.

Finally, the CTD web server was used to predict targeted drugs for key DE-ERSGs and identify small molecule compounds with potential therapeutic effects on OP patients. Bisphenol A, vinclozolin, arsenic acid sodium and so on eight kinds of drugs were associated with RPN2; 19 drugs such as cisplatin, adriamycin and ethanol were related to FOXO3. Four drugs (bisphenol A, cyclosporine, sodium arsenate and valproic acid) were associated with ERGIC2. Valproic acid, 4 diphenyl chloride and his two oxygen, potassium chromate (VI) and other three kinds of drugs was associated with MYO9A.

Sirt1-mediated FoxO deacetylation stimulates FoxO transcriptional activity and inhibits osteoclast formation.[49] Therefore, the antiosteoclast effect of FoxOs may be controlled by the Sirt1 stimulator. At present, many synthetic Sirt1 activators have been developed and shown to delay the progression of OP and osteoarthritis.[50] The first natural Sirt1 activator to be discovered was resveratrol (3,4',5-trihydroxystilbene).[51] In cultured cells, resveratrol and other Sirt1 activators such asSRT1720 or SRT2104 promotes osteoblast differentiation and reduces osteoclast formation.[52,53]

But there are still some shortcomings in our research. First, osteoporosis is not only caused by itself, but may also be affected by other physiological changes that come with aging, and age differences may lead to differences in gene expression in the study. And lifestyle factors, such as diet, exercise, smoking and alcohol consumption, can affect gene expression. Although the above confounding factors have been taken into account as much as possible in this study's data analysis, it may be difficult to completely eliminate their influence. Therefore, future studies could further explore the specific relationship between these confounding factors and ERS related gene expression with additional datasets to provide a deeper understanding. Secondly, this study verified the expression of key ERS-related genes in osteoporosis patients through RT-qPCR, but the sample size was limited. Future studies could expand the sample size to further validate and extend these findings. And we can further explore RPN2, FOXO3, The expression and possible role of ERGIC2 and MYO9A on cell types such as osteocyte, osteoma, osteoclast, and osteoblast activity in the bone microenvironment within the basic multicellular unit (BMU) and the specific role of these genes in the regulation of bone homeostasis were further validated by animal models or cell experiments. The potential of these genes as therapeutic targets for diseases such as osteoporosis can also be explored through the effects of gene knockout or overexpression on bone metabolism.

In summary, this study identified RPN2, FOXO3, ERGIC2 and MYO9A as biomarkers associated with ERS and OP through bioinformatics analysis, and further validated these genes through clinical trials. In addition, using the CTD web server to predict the targeted therapeutic drugs of key genes may provide new biological targets and therapeutic ideas for clinical treatment.

Abbreviations

OP, osteoporosis; MD, bone mineral density; EGs, differentially expressed genes; ERS, endoplasmic reticulum stress; GEO, Gene Expression Omnibus; WGCNA, weighted gene co-expression network analysis; DE-ERSGs, differentially expressed ERS-related genes; GO, Gene Ontology; BP, biological progress; CC, cellular component; MF, molecular function; KEGG, Kyoto Encyclopedia of Genes and Genomes; ROC, receiver operating characteristic; AUC, area under the curve; CTD, comparative toxicogenomics database; RT-qPCR, reverse transcription quantitative PCR; GSEA, gene set enrichment analysis.

Data Sharing Statement

The datasets (GSE56815 and GSE62402) analyzed during the current study are available in the Gene Expression Omnibus (GEO) database (https://www.ncbi.nlm.nih.gov/geo/).

Ethics Approval and Consent to Participate

Approval was granted by the Beijing Jishuitan Hospital Guizhou Hospital ethics committee (approval number: 20221208). Informed consent was obtained from all individual participants included in the study.

Consent for Publication

The authors affirm that human research participants provided informed consent for publication of the images in Figure 6.

Acknowledgments

We thank the patients for their cooperation and continued support for this study.

Author Contributions

All authors made significant contributions to the work of the report, whether in conception, study design, execution, data acquisition, analysis and interpretation; Participate in the drafting, revision, or critical review of articles; Final approval

of the publication version; Agree with the journal to which the article was submitted; And agree to take responsibility for all aspects of the job.

Funding

The authors declare that no funds, grants,or other support were received during the preparation of this manuscript.

Disclosure

The authors declare that they have no competing interests.

References

1. Iolascon G, de Sire A, Curci C. et al. Osteoporosis guidelines from a rehabilitation perspective: systematic analysis and quality appraisal using AGREE II. *Eur J Phys Rehabil Med*. 2021;57(2):273–279. doi:10.23736/S1973-9087.21.06581-3
2. Blake J, Cosman FA, Lewiecki EM, McClung MR, Pinkerton J, Shapiro M. Management of osteoporosis in postmenopausal women: the 2021 position statement of The North American Menopause Society. *Menopause*. 2021;28(9):973–997. doi:10.1097/GME.0000000000001831
3. Lin XC, Wu JJ, Huang HX, et al. Problems and strategies of osteoporosis prevention and treatment at the grassroots level in China. *ChinJ Osteoporosis*. 2022;28:16.
4. Oslowski CM, Urano F. Measuring ER stress and the unfolded protein response using mammalian tissue culture system. *Methods Enzymol*. 2011;490:71–92.
5. Sicari D, Delaunay-Moisan A, Combettes L, Chevet E, Igbaria A. A guide to assessing endoplasmic reticulum homeostasis and stress in mammalian systems. *Febs j*. 2020;287(1):27–42. doi:10.1111/febs.15107
6. Anelli T, Sitia R. Protein quality control in the early secretory pathway. *EMBO j*. 2008;27(2):315–327. doi:10.1038/sj.emboj.7601974
7. Chadwick SR, Lajoie P. Endoplasmic reticulum stress coping mechanisms and lifespan regulation in health and diseases. *Front Cell Dev Biol*. 2019;7:84. doi:10.3389/fcell.2019.00084
8. Oakes SA, Papa FR. The role of endoplasmic reticulum stress in human pathology. *Annu Rev Pathol*. 2015;10(1):173–194. doi:10.1146/annurev-pathol-012513-104649
9. Li SH, Zhang TS, Xing KY, He XZ, Li YW. Significance of overexpression of transcriptional activator 4 in osteoporosis induced by endoplasmic reticulum overstress. *J Spinal Surg*. 2019;19:259–264.
10. Guo JC. Mechanism of endoplasmic reticulum stress signaling molecule PERK regulating osteoclast differentiation and function. *Huazhong Univ Sci Tech*. 2022.
11. Al-Barghouthi BM, Farber CR. Dissecting the genetics of osteoporosis using systems approaches. *Trends Genet*. 2019;35(1):55–67. doi:10.1016/j.tig.2018.10.004
12. Langfelder P, Horvath S. WGCNA: an R package for weighted correlation network analysis. *BMC Bioinf*. 2008;9(1):559. doi:10.1186/1471-2105-9-559
13. Tian Z, He W, Tang J, et al. Identification of important modules and biomarkers in breast cancer based on WGCNA. *Onco Targets Ther*. 2020;13:6805–6817. doi:10.2147/OTT.S258439
14. Ritchie ME, Phipson B, Wu D, et al. limma powers differential expression analyses for RNA-sequencing and microarray studies. *Nucleic Acids Res*. 2015;43(7):e47. doi:10.1093/nar/gkv007
15. Chen H, Boutros PC. VennDiagram: a package for the generation of highly-customizable Venn and Euler diagrams in R. *BMC Bioinf*. 2011;12(1):35. doi:10.1186/1471-2105-12-35
16. Wu T, Hu E, Xu S, et al. clusterProfiler 4.0: a universal enrichment tool for interpreting omics data. *Innovation*. 2021;2(3):100141. doi:10.1016/j.xinn.2021.100141
17. Hänzelmann S, Castelo R, Guinney J. GSVA: gene set variation analysis for microarray and RNA-seq data. *BMC Bioinf*. 2013;14(1):7. doi:10.1186/1471-2105-14-7
18. Robin X, Turck N, Hainard A, et al. pROC: an open-source package for R and S+ to analyze and compare ROC curves. *BMC Bioinf*. 2011;12(1):77. doi:10.1186/1471-2105-12-77
19. William Revelle. *Psych: Procedures for Psychological, Psychometric, and Personality Research* R package version 2.4.3. Evanston, Illinois: Northwestern University; 2024.
20. Ensrud KE, Crandall CJ. Osteoporosis. *Ann Intern Med*. 2017;167:Itc17–itc32.
21. Compston JE, McClung MR, Leslie WD. Osteoporosis. *Lancet*. 2019;393(10169):364–376. doi:10.1016/S0140-6736(18)32112-3
22. Hamamura K, Yokota H. Stress to endoplasmic reticulum of mouse osteoblasts induces apoptosis and transcriptional activation for bone remodeling. *FEBS Lett*. 2007;581(9):1769–1774. doi:10.1016/j.febslet.2007.03.063
23. Chen Y, Gao H, Yin Q, et al. ER stress activating ATF4/CHOP-TNF-α signaling pathway contributes to alcohol-induced disruption of osteogenic lineage of multipotential mesenchymal stem cell. *Cell Physiol Biochem*. 2013;32(3):743–754. doi:10.1159/000354476
24. Sekiya H, Murakami T, Saito A, et al. Effects of the bisphosphonate risedronate on osteopenia in OASIS-deficient mice. *J Bone Miner Metab*. 2010;28(4):384–394. doi:10.1007/s00774-009-0142-y
25. Zhang P, Hamamura K, Jiang C, Zhao L, Yokota H. Salubrinal promotes healing of surgical wounds in rat femurs. *J Bone Miner Metab*. 2012;30(5):568–579. doi:10.1007/s00774-012-0359-z
26. Potier E, Noailly J, Ito K. Directing bone marrow-derived stromal cell function with mechanics. *J Biomech*. 2010;43(5):807–817. doi:10.1016/j.jbiomech.2009.11.019
27. Han C, Xie K, Yang C, et al. HA15 alleviates bone loss in ovariectomy-induced osteoporosis by targeting HSPA5. *Exp Cell Res*. 2021;406(2):112781. doi:10.1016/j.yexcr.2021.112781

28. Crimaudo C, Hortsch M, Gausepohl H, Meyer DI. Human ribophorins I and II: the primary structure and membrane topology of two highly conserved rough endoplasmic reticulum-specific glycoproteins. *EMBO j*. 1987;6(1):75–82. doi:10.1002/j.1460-2075.1987.tb04721.x
29. Hortsch M, Avossa D, Meyer DI. Characterization of secretory protein translocation: ribosome-membrane interaction in endoplasmic reticulum. *J Cell Biol*. 1986;103(1):241–253. doi:10.1083/jcb.103.1.241
30. Kelleher DJ, Kreibich G, Gilmore R. Oligosaccharyltransferase activity is associated with a protein complex composed of ribophorins I and II and a 48 kd protein. *Cell*. 1992;69(1):55–65. doi:10.1016/0092-8674(92)90118-V
31. Kelleher DJ, Gilmore R. An evolving view of the eukaryotic oligosaccharyltransferase. *Glycobiology*. 2006;16(4):47r–62r. doi:10.1093/glycob/cwj066
32. Ni L, Yu J, Gui X, et al. Retracted: overexpression of RPN2 promotes osteogenic differentiation of hBMSCs through the JAK/STAT3 pathway. *FEBS Open Bio*. 2020;10(1):158–167. doi:10.1002/2211-5463.12766
33. Chen D, Gong Y, Xu L, Zhou M, Li J, Song J. Bidirectional regulation of osteogenic differentiation by the FOXO subfamily of Forkhead transcription factors in mammalian MSCs. *Cell Prolif*. 2019;52(2):e12540. doi:10.1111/cpr.12540
34. Renault VM, Rafalski VA, Morgan AA, et al. FoxO3 regulates neural stem cell homeostasis. *Cell Stem Cell*. 2009;5(5):527–539. doi:10.1016/j.stem.2009.09.014
35. Furuyama T, Kitayama K, Yamashita H, Mori N. Forkhead transcription factor FOXO1 (FKHR)-dependent induction of PDK4 gene expression in skeletal muscle during energy deprivation. *Biochem J*. 2003;375(2):365–371. doi:10.1042/bj20030022
36. Ambrogini E, Almeida M, Martin-Millan M, et al. FoxO-mediated defense against oxidative stress in osteoblasts is indispensable for skeletal homeostasis in mice. *Cell Metab*. 2010;11(2):136–146. doi:10.1016/j.cmet.2009.12.009
37. van der Vos KE, Coffer PJ. FOXO-binding partners: it takes two to tango. *Oncogene*. 2008;27(16):2289–2299. doi:10.1038/onc.2008.22
38. Jasreen K, Jennifer T, Shek M, et al. An overview of the regulation of bone remodelling at the cellular level. *Clin Biochem*. 2012;45(12):863–873. doi:10.1016/j.clinbiochem.2012.03.021
39. Zhu C, Shen S, Zhang S, Huang M, Zhang L, Chen X. Autophagy in bone remodeling: a regulator of oxidative stress. *Front Endocrinol (Lausanne)*. 2022;13:898634. doi:10.3389/fendo.2022.898634
40. Xiao L, Ma P, Su C, et al. The roles of FoxO transcription factors in regulation of bone cells function. *Int J Mol Sci*. 2020;21(3):692. doi:10.3390/ijms21030692
41. Kwok SC, Liu X, Daskal I. Molecular cloning, expression, localization, and gene organization of PTX1, a human nuclear protein that is downregulated in prostate cancer. *DNA Cell Biol*. 2001;20(6):349–357. doi:10.1089/10445490152122460
42. Kwok SC, Kumar S, Dai G. Characterization of a Variant of ERGIC2 Transcript. *DNA Cell Biol*. 2014;33(2):73–78. doi:10.1089/dna.2013.2225
43. Lanctôt C, Moreau A, Chamberland M, Tremblay ML, Drouin J. Hindlimb patterning and mandible development require the Ptx1 gene. *Development*. 1999;126(9):1805–1810. doi:10.1242/dev.126.9.1805
44. O'Connor E, Phan V, Cordts I, et al. MYO9A deficiency in motor neurons is associated with reduced neuromuscular agrin secretion. *Hum Mol Genet*. 2018;27(8):1434–1446. doi:10.1093/hmg/ddy054
45. Ohno K, Ohkawara B, Shen XM, Selcen D, Engel AG. Clinical and pathologic features of congenital myasthenic syndromes caused by 35 genes-a comprehensive review. *Int J Mol Sci*. 2023;25(1):24. doi:10.3390/ijms25010024
46. Bayram Y, Karaca E, Coban Akdemir Z, et al. Molecular etiology of arthrogryposis in multiple families of mostly Turkish origin. *J Clin Invest*. 2016;126(2):762–778. doi:10.1172/JCI84457
47. Su Y, Yu G, Li D, et al. Identification of mitophagy-related biomarkers in human osteoporosis based on a machine learning model. *Front Physiol*. 2023;14:1289976. doi:10.3389/fphys.2023.1289976
48. Ma Z, Wei Y, Zhang L, et al. GCTOF-MS Combined LC-QTRAP-MS/MS reveals metabolic difference between osteoarthritis and osteoporotic osteoarthritis and the intervention effect of erxian decoction. *Front Endocrinol (Lausanne)*. 2022;13:905507. doi:10.3389/fendo.2022.905507
49. Kim HN, Han L, Iyer S, et al. Sirtuin1 suppresses osteoclastogenesis by deacetylating FoxOs. *Mol Endocrinol*. 2015;29(10):1498–1509. doi:10.1210/me.2015-1133
50. Bonkowski MS, Sinclair DA. Slowing ageing by design: the rise of NAD(+) and sirtuin-activating compounds. *Nat Rev Mol Cell Biol*. 2016;17(11):679–690. doi:10.1038/nrm.2016.93
51. Howitz KT, Bitterman KJ, Cohen HY, et al. Small molecule activators of sirtuins extend Saccharomyces cerevisiae lifespan. *Nature*. 2003;425(6954):191–196. doi:10.1038/nature01960
52. Shakibaei M, Buhrmann C, Mobasheri A. Resveratrol-mediated SIRT-1 interactions with p300 modulate receptor activator of NF-kappaB ligand (RANKL) activation of NF-kappaB signaling and inhibit osteoclastogenesis in bone-derived cells. *J Biol Chem*. 2011;286(13):11492–11505. doi:10.1074/jbc.M110.198713
53. GurtI, ArtsiH, Cohen-KfirE, et al. The Sirt1 Activators SRT2183 and SRT3025 Inhibit RANKL-induced osteoclastogenesis in bone marrowderived macrophages and down-regulate Sirt3 in Sirt1 null cells. *PLoS One*. 2015;10(7):e0134391. doi:10.1371/journal.pone.0134391